- Technical Paper -

EXPERIMENTAL INVESTIGATION ON FERRO-CEMENT LAMINATED MASONRY INFILLED RC FRAME AND CAPACITY EVALUATION

Debasish SEN[*1], Hamood ALWASHALI[*2], Masaki MAEDA[*3] and Matsutaro SEKI[*4]

ABSTRACT

Ferro-cement application on masonry infilled RC building is a low cost strengthening technique. However, seismic performance of structure after Ferro-cement strengthening has not been comprehensively investigated yet, especially focusing on load transfer mechanism. This study aims to investigate effect of wire mesh ratio on seismic performance, i.e. strength and failure mechanism, of two half-scaled Ferro-cement laminated masonry infilled RC frames. Simple prediction model of observed failure mechanisms has also been proposed and verified using experimental results.

Keywords: RC frame, Ferro-cement, Wire mesh, Masonry infill, Seismic strengthening.

1. INTRODUCTION

Seismic strengthening of vulnerable RC buildings is one of the most important concern for structural engineers, especially in developing countries, because of the severe damages and large number of injuries occurred during past earthquakes, such as Nepal Earthquake 2015. RC buildings with masonry infill are one of the most popular structures in developing countries. Generally, masonry infill walls are used as partition and commonly considered non-structural elements. In this context, strengthening of existing non-structural component of RC frame, i.e. infill masonry, and utilizing it as structural element would be a feasible and low cost solution. As a low cost strengthening material, several researchers [1-6] used Ferro-cement to strengthen masonry infilled RC frame. In general, Ferro-cement [FC] retrofitting of masonry refers to the application of an initial mortar layer on the both faces of masonry wall which is followed by the placement of steel wire mesh and a second mortar layer, as shown in Fig.1. Anchorages are also being used to attach wire mesh to masonry and/or RC frame. Though, Ferro-cement has been studied for decades as a construction material, there is no design specification of FC (e.g. amount of mesh reinforcement, mortar thickness etc.) which can be used for shear strengthening of unreinforced infilled masonry. In addition, all of the previous studies [1-4,6] mainly focused on in-plane capacity improvement of relatively low strength infill masonry (compressive strength 6~15MPa), rather than focusing on load transfer mechanism i.e. failure mode evaluation. Most of the previous studies, explained failure mode as crushing or shear cracking of FC laminated masonry infill, which is similar to infill masonry. However, the failure of surrounding RC frame might not be exactly similar as masonry infilled RC frame, i.e. formation of flexural hinge, because stiffness and strength of FC laminated infill masonry is much higher than that of infill masonry, which has been completely overlooked.

Considering the aforementioned lack of studies, this study aims to experimentally investigate effect of wire mesh steel area ratio on lateral behaviour, especially failure mechanism and strength, of FC laminated masonry infilled RC frame. In addition, current study also aims to clarify all possible failure modes, and subsequently propose and validate lateral strength capacity evaluation model of observed failure modes in the experimental program.

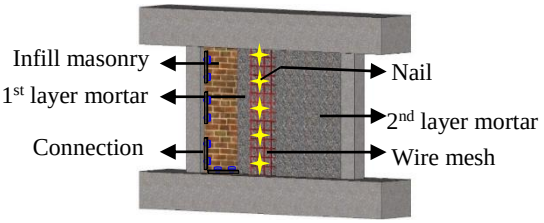

Fig. 1: Schematic diagram of FC lamination on masonry infill

2. EXPERIMENTAL PROGRAM

2.1 Specimen design concept

In this study, primarily experimental results of several half scaled masonry infilled RC frames, with and without Ferro-cement strengthening, have been acquired from literature [1-6] to get an idea about the practices in research field. All the studied FC laminated masonry walls contain square wire mesh on solid or hollow bricks. The shear stress on FC lamination (τ_{FC}) has been computed in reference to Fig. 2, where, P_1, P_2 = experimental lateral capacity of un-strengthened and strengthened specimen; n_s = number of strengthened surfaces; L= length of masonry; and t_{FC} = thickness of

*1 Graduate School of Engineering, Tohoku University, JCI Student Member
*2 Assistant Prof., Dept. of Architecture and Building Science, Tohoku University, Dr. Eng., JCI Member
*3 Professor, Dept. of Architecture and Building Science, Tohoku University, Dr. Eng., JCI Member
*4 Visiting Research Fellow, Building Research Institute, Dr. Eng.

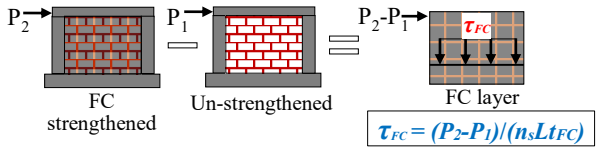

Fig. 2: Contribution of ferro-cement layer

ferrocement layer. The shear stress on FC laminate (τ_{FC}) is presented in Fig. 3 as a function of normalized horizontal mesh reinforcement area (ρ_{wm}= A_{hs}/A_{mas}, where A_{hs} = total cross sectional area of horizontal mesh reinforcement, and A_{mas} = horizontal cross sectional area of masonry (length x thickness)). As shown in Fig. 3, the previous studies had horizontal mesh reinforcement between 0.05~0.35% of the horizontal masonry area. The shear stress on FC layer varied greatly between specimens. This large variation might be due to variation of failure modes, materials, and connections. In other words, wire mesh might not provide shear strength in a linear manner with the increase of wire mesh, rather it perhaps depends on the interaction between FC laminated infill and surrounding RC frame.

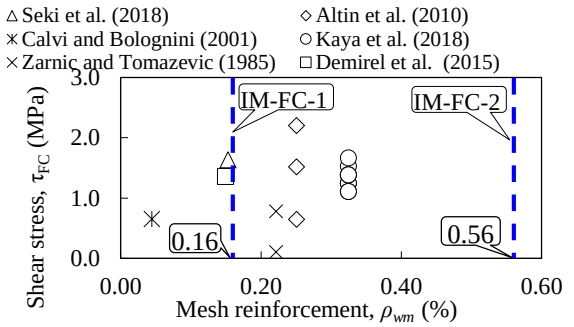

Fig. 3: Shear strength of FC layer as a function of mesh reinforcement ratio

As mentioned earlier, one of the objectives of this study is to investigate effect of wire mesh ratio on failure mechanism and strength of FC laminated masonry infilled RC frame. Therefore, wire mesh ratio for current study have been set to 0.16% (relatively low ratio) for specimen IM-FC-1 and 0.56% (relatively high ratio) for specimen IM-FC-2. For specimen IM-FC-2 wire mesh ratio has been set 0.56%, almost 3.5 times than specimen IM-FC-1, to investigate the effect of higher wire mesh ratio on the failure mechanism of surrounding RC frame. It is worthy to note that in this study FC has been applied on relatively strong masonry (compressive strength > 25 MPa) for strengthening purpose to understand effect on surrounding RC frame's damage.

2.2 Specimen details

Two half scaled masonry infilled RC frames have been constructed and infill masonry has been strengthened with Ferro-cement. The overall geometry of RC frame is shown in Fig. 4(a). Details of all specimens are shown in Table 1. The construction procedure of specimens is as follow: First, RC frame has been constructed and then masonry panel has been built inside frame, with solid bricks of 210x100x60 mm, in running bond manner. After seven days of masonry construction, 10mm thick mortar has been mounted on both faces of masonry wall. This is followed by attachment of square wire mesh to RC frame and masonry wall. The wire mesh has been connected to both columns and beams with bolt (inserted into pre-installed thread) and steel plate. The connection with column with bolt and steel plate is illustrated in Fig. 4(b)-(c), same connection method has been utilized with top and bottom beam also. In addition, the wire mesh has been connected with masonry infill by 32mm nails to hold the wire mesh in place during application of second layer mortar. The nails have been placed in drilled holes at a horizontal and vertical center to center distance of 250mm and 500mm, respectively. After seven days, second layer of mortar, having 15mm thickness, has been applied on wire mesh.

2.3 Material properties

The material tests have been conducted for each specimen as per Japanese standard [7]. The wire mesh has been tested as per ACI 549[8]. The mechanical properties of concrete, reinforcing steel, masonry, mortar and wire mesh are shown in Table 2.

2.4 Instrumentation and Loading

Both specimens have been subjected to cyclic lateral loading and 200kN constant vertical loads (N') on each column where axial load ratio ($N'/f_c bd$) is about 0.2. The schematic diagram of the loading system is shown

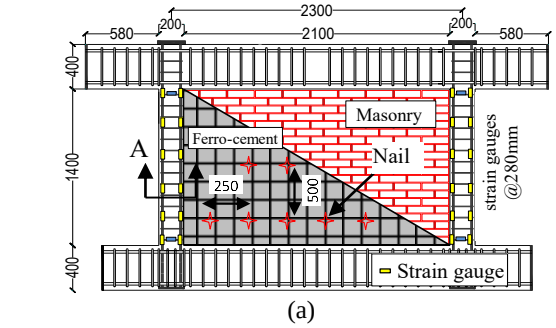

(a)

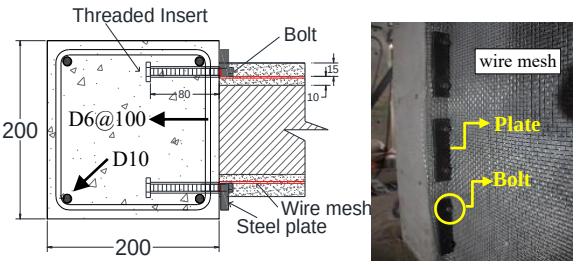

Section A-A

(b) (c)

Fig. 4: (a) Geometry of masonry infilled RC frame (b) and (c) connection of wire mesh to column

Table 1: Details of Specimen

Specimen	Column (mm)	Wire mesh		
		φ (mm)	s (mm)	ρ_{wm} (%)
IM-FC-1	200x200	0.9	5.45	0.16
IM-FC-2		1.6	4.75	0.56

φ = wire diameter, s= spacing and ρ_{wm} =Mesh reinforcement

Table 2: Material Properties (all values are in MPa)

Specimen	f_c'	f_y	f_{mas}	$f_{mor,j}$	$f_{mor,FC}$	$f_{u,wm}$
IM-FC-1	24	350	27	37	26	378
IM-FC-2	26		29	35	29	318

f_c'= concrete compressive strength, f_y/ $f_{u,wm}$ = yield/ ultimate strength of long reinforcement (D10) / wire mesh, f_{mas}= masonry compressive strength and $f_{mor,j}$ / $f_{mor,FC}$ = compressive strength of joint and FC mortar.

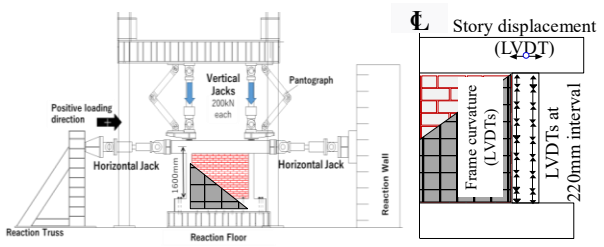

(a) (b)

Fig. 5: (a) Loading system and (b) position of LVDTs

in Fig. 5 (a), where two pantographs have been used to avoid out-of-plane movement of frame during loading. The cyclic lateral loading program consisted of two cycles for each lateral drift of 0.05, 0.1, 0.2, 0.4, 0.6, 0.8, 1.0, 1.5, and 2.0 %. The lateral drift is defined as the ratio of top lateral displacement, measured at the center of beam, to the height of column taken from the top of foundation beam to center of top beam. LVDTs were attached, as shown in Fig. 5(b), at the center of top beam and on both RC columns to measure top displacement and curvature of RC frame, respectively. Strain gauges have been attached on main reinforcements of both RC columns and shear reinforcements as shown in Fig. 4(a).

3. EXPERIMENTAL RESULTS

3.1 Cyclic lateral behavior and damages

IM-FC-1 (with lower wire mesh ratio i.e. 0.16%)

The hysteresis loops of IM-FC-1 is shown in Fig. 6(a). The response was essentially linear up to the formation of first crack on tension column at 0.05% story drift. At 0.1% story drift, longitudinal reinforcement yielded at the bottom of tensile column and it has been confirmed by checking strains (>2000μ) of the attached strain gauge at the bottom of column. At 0.2% story drift, flexural crack at the joint of strengthened wall and stub beam, as shown in Fig. 7(a), has also been observed. After cracking, the hysteresis loops began to open, specifically at the cycle of 0.4% story drift in which specimen reached to its maximum capacity and inclined crack appeared on the Ferro-cement laminated masonry. At around 0.6% drift, wire meshes started to be ruptured in the inclined crack which leads to sudden drop in lateral resistance. At this stage, sliding at the joint of strengthened wall and top beam has been started and also shear crack formed at the top of tension column. At about 1.5% story drift, direct / punching shear failure at top of the tension column, as shown in Fig. 7(a), has also been observed which has been confirmed by recorded strain values of the tie. Loading has been stopped at the 1st cycle of negative 2% lateral drift, where the bottom reinforcement of compression column buckled which is followed by cover concrete spalling. The final crack pattern under lateral cyclic loading is shown in Fig. 7(a).

IM-FC-2 (with higher wire mesh ratio i.e. 0.56%)

The hysteresis loops of IM-FC-2 is shown in Fig. 6(b). The response was also linear up to the formation of first crack on tension column at 0.05% lateral drift. The longitudinal reinforcements at the bottom of tension column experienced yielding at 0.1% story drift (checked using strain gauge). At 0.1~0.2% story drift, flexural crack at the joint of wall and stub beam, as shown in Fig. 7(b), has also been observed. After that, the width of tension crack at the bottom of column gradually increased up to 3mm. At about 1% story drift, core concrete of compression column started to crush. Wire meshes at the bottom of the wall, which have been connected directly to beam through steel plate and bolt, started to be ruptured at about 1.5% story drift. Loading has been finished at the 1st cycle of negative 2% lateral drift, where three main reinforcements of tension column ruptured. The final crack is shown in Fig. 7(b).

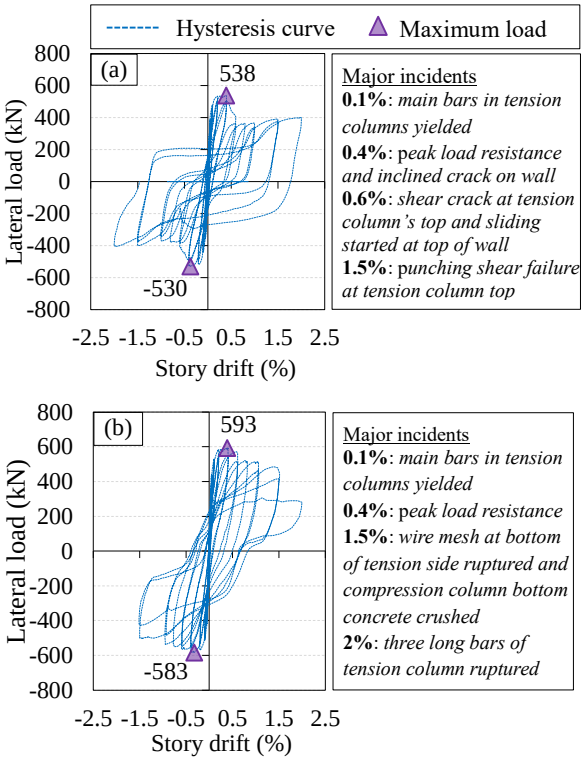

Fig. 6: Lateral load-story drift relationship of specimen (a) IM-FC-1, and (b) IM-FC-2

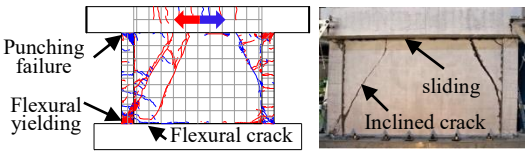

(a) Specimen IM-FC-1

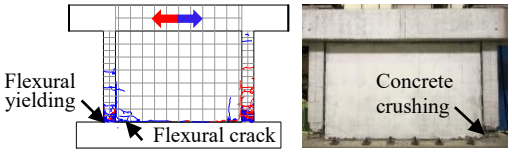

(b) Specimen IM-FC-2

Fig. 7: Crack pattern of specimens

3.2 Identification of failure mechanisms

Failure mode of structural wall, under lateral load, is mainly governed by shear, flexure or combination of the shear and flexure. The contribution of flexure and shear in top displacement is separated in the following process. Flexural deformation (Δ_{fl}) of RC frame was

measured using the LVDTs attached on the both RC columns as shown in Fig. 5(b). Total story deformation (Δ_{total}) was measured using the LVDTs attached on the top beam as shown in as shown in Fig. 5(b). This is followed by the determination of shear deformation (Δ_{sh}) at a certain drift using Eq. 1, assuming total deformation is the summation of shear and flexural deformation.

$$\Delta_{sh} = \Delta_{total} - \Delta_{fl} \quad (1)$$

where, Δ_{total}, Δ_{fl}, Δ_{sh} refer to total, flexural and shear deformation, respectively at the center of beam.

The obtained flexural and shear deformation in relation to the story drift are shown in Fig. 8(a)-(b). In specimen IM-FC-1, flexural contribution is relatively more at lower story drifts as shown in Fig. 8(a). At higher story drifts, tension column experienced direct punching shear failure following sliding at top joint which led to an increase in shear deformation. Another strengthened RC frame, namely IM-FC-2, experienced a flexure domination throughout course of the lateral drift as shown in Fig.8(b). In other word, IM-FC-1 behaved as flexural wall at the drift lower than 0.4% and then failed in punching shear of column, but IM-FC-2 specimen behaved like a flexural wall for all story drifts (as shown in Fig. 9(a)). However, if bond at top construction joint fails, i.e. sliding, direct shear failure of tension column might happen as shown in Fig. 9(b).

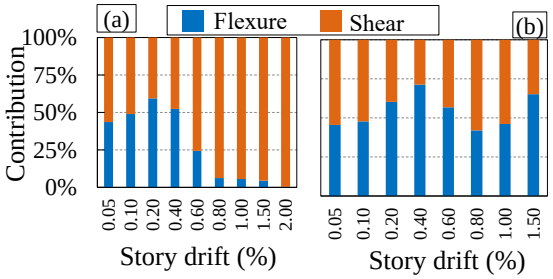

Fig.8: Shear and flexural contribution in story deformation of (a) IM-FC-1, and (b) IM-FC-2

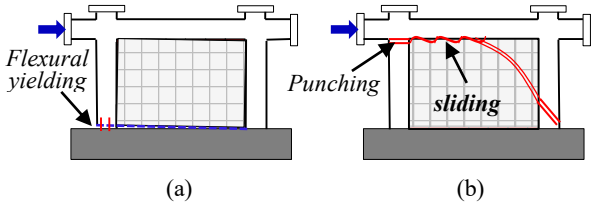

Fig. 9: (a) Flexural and (b) Column punching and joint failure of FC laminated specimens

3.3 Comparison of lateral behavior

The backbone curves of FC laminated masonry infilled RC frames are shown in Fig. 10. Comparing the peak resistance, it can be summarized that wire mesh ratio did not affect the lateral strength much because at peak resistance load transfer mechanism has been mainly governed by flexure for both specimens. Specimen with 0.16% mesh ratio, IM-FC-1, showed 25% capacity drop after peak resistance due to bond failure at top joint following by sliding. The specimen with 0.56% mesh ratio IM-FC-2, showed very gradual post peak declination which indicates a relatively ductile behavior.

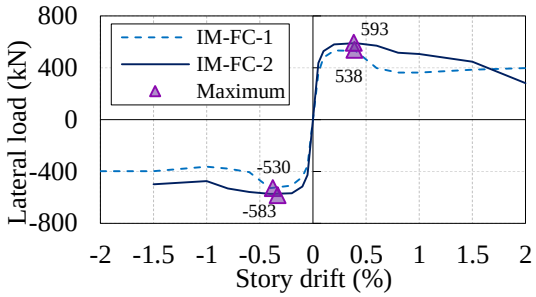

Fig. 10: Comparison of backbone curves

4. POSSIBLE FAILURE MODES

Generally, failure mode of masonry/concrete infilled RC frame depends on relative stiffness as well as strength of infill material compared to surrounding RC frame. In case of masonry infilled RC frame, infill masonry is the weakest part, therefore failure initiates on the masonry part. However, Ferro-cement laminated infill masonry has higher stiffness and strength compared to infill masonry. Therefore, RC frame could be the weakest part and consequently can fail as observed in the current experimental program. Meanwhile, crushing or cracking of FC laminated infill masonry is also evident in literature. Kaya et al. [1] investigated FC laminate masonry infilled RC frame where, crushing due to diagonal compression is evident as shown in Fig. 11(a). In addition, diagonal cracking of strengthened masonry is also evident in a study by Seki et al. [2], as shown in Fig. 11(b). In other studies [3-6], failure has not been clearly identified.

Based on the current experimental observation and previous studies [1-2] following four distinct failure modes, as shown in Fig. 12, have been identified. The lateral strength evaluation of Failure I and II, as observed in current study, is discussed in the following section.

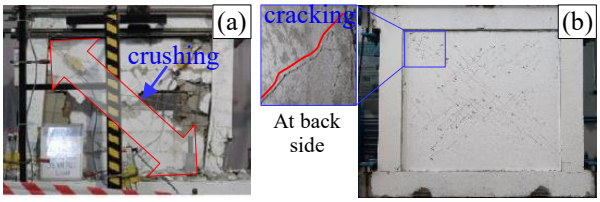

Fig. 11:(a) Diagonal compression [1] and (b) Diagonal cracking [2] of FC strengthened infilled masonry

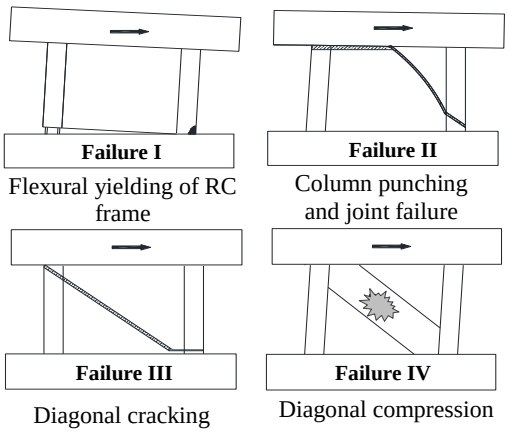

Fig. 12: All possible failure modes of Ferro-cement laminated masonry infilled RC frame

5. EVALUATION OF OBSERVED FAILURES

5.1 Failure I: Flexural yielding of RC frame

The lateral capacity at flexural yielding (Q_1), as shown in Fig. 13, of the FC laminated masonry infill in RC frame has been computed from flexural theory, using Eq. 2 and Eq. 3. It is to be noted that, in ultimate moment calculation (Eq. 3) the contribution of wire meshes has been ignored because wire meshes have been connected at intervals with stub beam. Therefore, the lateral capacity is provided by RC frame itself.

$$Q_1 = {}^{M_u}/_{h_o} \tag{2}$$

$$M_u = a_t f_y l_c + 0.5 N l_c \tag{3}$$

where, M_u = ultimate moment capacity of RC frame, h_o = clear height of column, a_t = cross sectional area of column longitudinal reinforcements, f_y= yield strength of column longitudinal reinforcement, l_c = c/c distance of boundary columns, N = Axial loads carried by both RC columns = $2N'$.

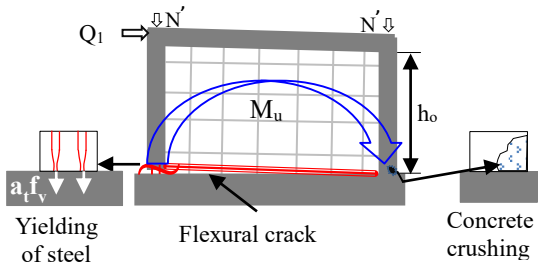

Fig. 13: Load transfer mechanism of flexural yielding of frame (Failure I)

5.2 Failure II: Column punching and top joint failure

Free body diagram of strengthened masonry infilled RC frame after top construction joint failure and column punching is shown in Fig. 14, which actually occurred in specimen IM-FC-1 at higher story drifts. The total shear capacity (Q_2) can be evaluated by Eq. 4.

$$Q_2 = {}_{ps}Q_c + {}_{js}Q_w + {}_{f}Q_c \tag{4}$$

where, ${}_{ps}Q_c$ = punching shear resistance of tension column, ${}_{js}Q_w$ = shear resistance at construction joint, and ${}_{f}Q_c$= flexural shear resistance of compression column.

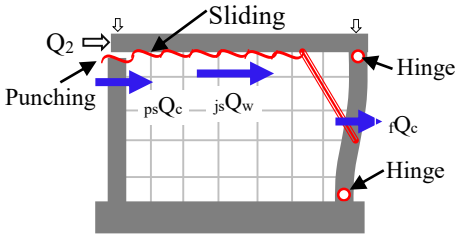

Fig. 14: Load transfer mechanism of column punching and joint failure (Failure II)

Punching shear capacity (${}_{ps}Q_c$) of tension column, and lateral capacity of compression column (${}_{f}Q_c$) of RC column can be computed as per JBDPA 2001[9] using Eq. (5) and Eq. (6), respectively. The source of joint shear capacity (${}_{js}Q_w$) could be the masonry joint mortar, mortar of FC layer and embedded wire meshes in FC layer. From the lateral behavior of specimen IM-FC-1, it is clear that initially shear strength is greater than flexural capacity (i.e. shear failure after flexural yielding) and the lateral resistance degraded 25% after occurring slippage at the top construction joint. This indicates that initially the bond between FC laminated masonry and soffit was working. Then, after slippage, wire meshes were working as dowel to provide residual capacity. Therefore, at initial stage, before any slippage at the interface of infill top and soffit, shear capacity can be considered as shear strength (cohesion) of mortar at interface. In initial bond capacity, wire mesh might have contribution in addition to mortar cohesion however, as a conservative approach wire mesh contribution has been ignored. After the occurrence of slippage wire mesh will be subjected to shearing force hence considered as the source of residual shear capacity at the interface. After slippage, friction might also work, however, has not been considered here for simplicity. The initial and residual joint shear capacity can be evaluated from Eq. 7 and Eq. 8, respectively.

$${}_{ps}Q_c = K_{min}\tau_o bD \tag{5}$$

$${}_{f}Q_c = \frac{2M_c}{h_o} \tag{6}$$

$${}_{js}Q_{wi} = \tau_{mas} l_w t_{mas} + \tau_{mor,FC} l_w n_s t_{FC} \tag{7}$$

$${}_{js}Q_{wr} = \sum a_{wm}\, \tau_{y,wm} \tag{8}$$

where, K_{min} = 0.34/(0.52+a/D), a = shear span = D/3, τ_o = shear strength of tension column, b and D = width and depth of column, M_c = ultimate moment capacity of column, h_o= clear height of column, ${}_{js}Q_{wi}$ = initial shear capacity at joint, ${}_{js}Q_{wr}$ = residual shear capacity at joint, $\tau_{mas}/\tau_{mor,FC}$ = shear strength (cohesion) of mortar in masonry joint and Ferro-cement, l_w = length of infill, t_{mas}/t_{FC} = thickness of masonry wall and FC layer, n_s = number of FC surface, a_{wm} = cross sectional area of wire mesh, $\tau_{y,wm}$ = shear strength of wire mesh ($f_{y,wm}/\sqrt{3}$),. It is to be noted that cohesion capacity of mortar, for both masonry and FC layer, has been considered as $0.17\sqrt{f_{mor}}$, (f_{mor} =compressive strength of mortar), which has been recommended by Namaan 2000 [10], and Mander and Nair 1994 [11] as shear strength of FC. The yield strength of wire mesh, ($f_{y,wm}$ = 0.925*$f_{u,wm}$) has been considered as per AS/NZS [12].

6. VALIDATION OF CAPACITY EVALUATION

In this section, capacity prediction models of Failure mode I (flexural yielding of RC frame) has been validated using experimental observation of specimen IM-FC-1 and IM-FC-2 as shown in Fig.15(a)-(b) and Table 3. Since, in specimen IM-FC-1 column punching and top joint failure did not occur at peak resistance therefore residual capacity of Failure mode II (column punching and top joint failure) has been compared with experimental results of specimen IM-FC-1.

It is evident by comparing experimental and calculated values (Eq.2), that the flexural capacity without considering wire mesh can give fair approximation of lateral load capacity of FC retrofitted masonry infilled RC frame.

Table 3: Lateral capacity of specimens

Lateral capacity (kN)		Specimen	
		IM-FC-1	IM-FC-2
Experimental	Peak (avg.)	534	588
	Residual (avg.)	373	-
Flexural capacity, Q_1		494	494
Initial shear capacity, Q_2		487	485
Residual shear capacity, $Q_{2,residual}$		278	481

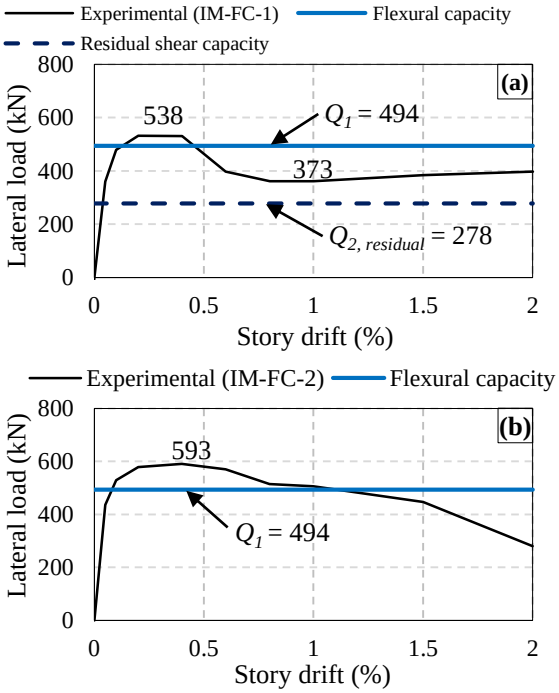

Fig. 15: Calculated capacity and envelop load-story drift curve of (a) IM-FC-1 and (b) IM-FC-2

For both specimens (IM-FC-1 and IM-FC-2) peak resistance has been governed by flexural yielding of RC frame, therefore initial lateral capacity of Failure mode II (column punching and top joint failure) should be greater that flexural yielding capacity (Failure mode I). However, the calculated initial capacities are close to the calculated flexural capacities. This can be attributed to the ignorance of wire mesh contribution in bond capacity, which need further study.

The post peak response of specimen IM-FC-1 has been governed by the punching shear of tension column hence the residual shear capacity can be evaluated. The plot on Fig. 15(a) also shows that the proposed estimation method gave a conservative prediction of residual shear resistance which could be attributed to the friction at the interface which has not been considered.

7. CONCLUSIONS

In this study, an experimental investigation has been conducted on the lateral behavior of two Ferro-cement laminated infilled RC frame with varying wire mesh steel area ratio. The following conclusions can be drawn from this study-

a) The observed failure mechanism at the peak resistance, of the studied Ferro-cement laminated specimens, with 0.16% and 0.56% mesh ratio, were flexural yielding of RC frame which has been completely ignored in literature.

b) Since, Ferro-cement laminated masonry walls did not crack diagonally and failure mechanism at peak was flexural yielding, therefore wire mesh ratio, 0.16% and 0.56%, did not strongly affect the lateral capacity of Ferro-cement strengthened masonry infilled RC frame.

c) Based on current study and past studies, four possible failure modes have been identified.

d) Lateral capacity estimation method for the failure modes observed in this study has been proposed and verified, with fare agreement.

Further experimental studies are required to confirm the possible failure modes identified here as well as to confirm capacity evaluation methods.

ACKNOWLEDGEMENT

This research is supported by SATREPS project "Technical Development to Upgrade Structural Integrity of Buildings in Densely Populated Urban Areas and its Strategic Implementation towards Resilient Cities (TSUIB)" (principle investigators: Prof. Yoshiaki Nakano, U. Tokyo and Mr. Mohammad Shamim Akhter, HBRI, Bangladesh) and JSPS KAKENHI Grant Number JP18H01578 (Principal investigator: Prof. Masaki Maeda, Tohoku University).

REFERENCES

[1] Kaya, F., Tekeli, H., and Anil, Ö.: Experimental behavior of strengthening of masonry infilled reinforced concrete frames by adding rebar-reinforced stucco, Struc. Conc., pp. 1-14, 2018.2

[2] Seki, M., Popa, V., Lozinca, E., Dutu, A., and Papurcu, A.: Experimental study on retrofit technologies for RC frames with infilled brick masonry walls in developing countries, In Proc. of 16th ECEE, Greece, 2018.6

[3] Demirel, I. O., Yakut, A, Binici, B. and Canbay, E.: An Experimental Investigation of Infill Behaviour in RC Frames, In Proc. of the 10th PCEE, Australia, 2015.11

[4] Altın, S., Anıl, Ö., Kopraman, Y., and Belgin, Ç.: Strengthening masonry infill walls with reinforced plaster, In Proc. of the Institution of Civil Engineers-Structures and Buildings, 163, pp. 331-342, 2010

[5] Calvi, G. M., & Bolognini, D.: Seismic response of reinforced concrete frames infilled with weakly reinforced masonry panels, Jour. of Earthq. Engg., Vol. 5, pp. 153-185, 2001

[6] Žarnić, R., and Tomaževič, M.: Study of the behaviour of masonry infilled reinforced concrete frames subjected to seismic loading, 1985.

[7] Japanese Standard Association. Jap. Industrial Standards. 2010.

[8] ACI 549 1R-93, Guide for the Design, Construction and Repair of Ferro-cement, 1993 (Reapproved 1999)

[9] Japan Building Disaster Prevention Association, Standard for seismic evaluation of existing conc. Buildings, 2001

[10] Naaman, A. E. Ferrocement and laminated cementitious composites, Techno press,2000

[11] Mander, J. B., & Nair, B. Seismic resistance of brick-infilled steel frames with and without retrofit. The Masonry Journal, 12(2), 24-37,1994.

[12] AS/NZS 4671: Steel reinforcing materials,2001